Journal of Catalysis 278 (2011) 133–142

Contents lists available at ScienceDirect

Journal of Catalysis

journal homepage: www.elsevier.com/locate/jcat

CO oxidation on phosphate-supported Au catalysts: Effect of support reducibility on surface reactions

Meijun Li, Zili Wu, S.H. Overbury *

Chemical Sciences Division, Oak Ridge National Laboratory, Oak Ridge, TN 37831, United States

ARTICLE INFO

Article history:
Received 16 July 2010
Revised 23 November 2010
Accepted 28 November 2010
Available online 7 January 2011

Keywords:
Au catalyst
$FePO_4$
$LaPO_4$
CO adsorption
Catalytic CO oxidation
FTIR
Raman spectroscopy
Mechanism

ABSTRACT

Previous work has shown that Au supported on $FePO_4$ can be stable and active for CO oxidation and that oxygen from the $FePO_4$ can participate in the CO oxidation. In this paper, we have used gas transient DRIFTS-QMS, Raman, temperature-programmed reduction and CO oxidation activity measurements to compare adsorption and oxidation of CO on two comparably loaded Au catalysts supported on both a reducible phosphate support, $FePO_4$, and a non-reducible support, $LaPO_4$. H_2-TPR confirms that the Au/$FePO_4$ catalyst is highly reducible and that the reduction is strongly promoted by the Au, while neither $LaPO_4$ nor Au/$LaPO_4$ are reducible up to 500 °C. The nature of Au species was determined by CO adsorption. For Au/$FePO_4$, cationic Au is present after oxidative treatment, and metallic Au dominates after reductive treatment. The majority of the cationic Au observed on the $FePO_4$ support undergoes *in situ* reduction to metallic Au during rt CO adsorption. For Au/$LaPO_4$, no cationic Au is observed, but metallic Au is present after both oxidative and reductive treatment. In addition, metallic Au is accompanied by anionic Au, not seen on Au/$FePO_4$, which accumulates during CO exposure, even after an oxidative pretreatment. Unexpectedly, CO interacts rapidly with Au/$LaPO_4$ to evolve CO_2 and form both adsorbed CO_2 and "carbonate-like" species, even though the $LaPO_4$ is non-reducible and Raman fails to find evidence for loss of structural oxygen. H_2 coevolves with CO_2 during CO-TPR of Au/$LaPO_4$ (but not for Au/$FePO_4$) leading to the conclusion that surface hydroxyl is the source of oxygen during CO exposure to Au/$LaPO_4$. Anionic Au is associated with the vacancies remaining after reaction of hydroxyl with CO.

1. Introduction

Gold is now well known to be an active catalysts for CO oxidation which it can do well and selectively in the presence of H_2 [1]. For this reason, it is of potential use in cleanup of CO present in air or in H_2 fuel streams in fuel cell applications [2]. Au is also able to oxidize CO using H_2O, i.e. to catalyze the water–gas shift (WGS) reaction, a capability which may ultimately lead to commercial application [3–5]. Other catalytic uses for selective oxidation have also been examined [6]. Although its activity for these reactions can be very high, its performance and stability depends sensitively upon preparation conditions and the support used, and for this reason, it has been the subject of considerable interest during the past decade. Much debated are the oxidation state of Au in its active state and the reaction pathways and intermediates in CO oxidation and WGS. It is widely held that the support plays a role in mitigating these pathways and in affecting the oxidation state of the Au.

An important question in understanding the pathways for CO reaction is how O_2 is activated. Previous work shows that low-index Au single crystal surfaces such as Au(1 1 1) do not readily adsorb O_2 [7,8] or more accurately only weakly physisorb O_2 without dissociation. However, atomically or highly dispersed Au is apparently able to dissociate O_2, yielding adsorbed O atoms, suggesting that low-coordination Au sites are required [9]. Transient IR and isotope exchange experiments on catalysts containing highly dispersed Au clusters/nanoparticles on TiO_2 and Al_2O_3 have provided evidence that metallic Au clusters adsorb CO readily, but they do not adsorb much oxygen and the adsorbed oxygen is catalytically very active [10,11]. Experiments with isotopically labeled O_2 near room temperature (rt) indicate that reactant O_2 does not scramble, implying that all dissociated O_2 reacts rapidly with CO rather than to associatively recombine [12]. Theoretical analysis supported by DFT calculations [13,14] and analysis of experimental size-dependent measurements [15] suggest that low-coordination kink and edge sites are necessary for CO oxidation activity, presumably because these are the sites necessary for O_2 activation. Very specific structures of Au have been found experimentally that are highly active in CO oxidation [16], possibly for their ability to bind or activate O_2 [17]. Besides direct reaction between CO and dissociated O on Au particles, a second pathway that has been suggested for CO oxidation is through a CO–OH intermediate, referred to as carboxyl or hydroxycarbonyl. Carboxyl has been identified by DFT as a reactive intermediate, and the carboxyl-mediated route is

* Corresponding author.
E-mail address: overburysh@ornl.gov (S.H. Overbury).

0021-9517/$ - see front matter © 2010 Elsevier Inc. All rights reserved.
doi:10.1016/j.jcat.2010.11.019

suggested to be the dominant pathway for WGS on Cu surface [18]. Promotion of *CO oxidation* by H_2O or H_2 observed on Au catalysts has also been attributed to this carboxyl intermediate [10,19–21]. For Au on Al_2O_3 or TiO_2, promotion by H_2O cannot be attributed to WGS reaction [12] since WGS does not occur at the reaction temperature. Apparently, the H persists through many turnovers rather than react to evolve H_2. In these cases where hydroxyl is present either from adventitious water or from H_2 co-feed, this pathway may be an important contributor to CO conversion. Reaction by this mechanism may occur at a Au^+ site or may involve hydroxyl on the support or at the Au support interface, suggesting a role of the support in promoting CO oxidation. Another pathway for CO oxidation is one in which the support contributes oxygen through activation of O_2 and a redox cycle similar to a Mars–van Krevelen-type reaction. Although this pathway has been suggested for reducible supports such as Fe_2O_3 and TiO_2 [22], there is little positive evidence for this pathway occurring on oxide-supported Au catalysts.

Non-oxide supports, such as carbides [23,24] and phosphates [25–37], provide additional insight into possible roles of the support in promoting oxygen activation in CO oxidation. Gold nanoparticles can be well dispersed on some metal phosphate supports and show significant activity at rt. Recently, we reported the first observation that the presence of Au species assists the storage of active oxygen species in $FePO_4$, which opens up two channels for CO oxidation on $Au/FePO_4$ at rt: Mars–van Krevelen (redox) and direct (e.g. Langmuir–Hinshelwood) mechanisms [28]. To further explore this unexpected result, we have now performed comparative studies between the $Au/FePO_4$ catalysts and Au supported on a $LaPO_4$ support that is presumably non-reducible and therefore incapable of a redox pathway. Interestingly, we find that surface hydroxyls on the $LaPO_4$ open a pathway for CO oxidation in this catalyst system. In the following, we discuss studies of the effects of treatments in oxidizing and reducing environments (both H_2 and CO) and probe their effects upon the support, the Au nanoparticles and the CO oxidation reaction rates.

2. Experimental

2.1. Preparation of $Au/LaPO_4$ and $Au/FePO_4$

The $LaPO_4$ (surface area 56 m^2/g) and $FePO_4$ (surface area 28 m^2/g) supports were purchased from Aldrich. Au was emplaced onto $LaPO_4$ using deposition–precipitation (DP) with a $HAuCl_4$ precursor. Briefly, 0.6 g $HAuCl_4$ was dissolved in 100 ml deionized (DI) H_2O, the pH of the solution adjusted to 7 with KOH solution and 2.0 g $LaPO_4$ was added. The pH value of the solution dropped after adding $LaPO_4$ and was re-adjusted to approximately 7 by KOH solution. The suspension was stirred at 80 °C for 2 h and then filtered and washed with DI H_2O. The product was dried at 40 °C for two days and stored without further calcination in this "as-synthesized" state. TEM measurements on as-synthesized $Au/LaPO_4$ showed most Au particles less than 10 nm (Fig. S3a). Au loading was 5.8 wt% as determined by XRF analysis. $Au/FePO_4$ was synthesized as reported in previous papers, but with a lower Au wt loading of 2.5% as determined by ICP analysis on an IRIS Intrepid II XSP spectrometer (Thermo Electron Corporation). TEM measurements on as-synthesized $Au/FePO_4$ showed comparable Au particle size as on the $Au/LaPO_4$ (Fig. S3b).

2.2. Transient FTIR experiments

The chemisorption and reaction experiments were performed using a transient gas switching system for probing catalytic pathways. FTIR spectroscopy was conducted in a diffuse reflectance cell (cell volume about 6 cm^3) in a Nicolet Nexus 670 FTIR spectrometer using a MCT/A detector with a spectral resolution of 4 cm^{-1}. After the desired pretreatments, a background spectrum was collected from the sample using 256 scans and 4 cm^{-1} resolution. Diffuse reflectance FTIR spectra (DRIFTS) were obtained by subtracting the background spectrum from subsequent spectra and are reported herein. Gases leaving the DRIFTS cell were analyzed using a downstream gas sampling quadrupole mass spectrometer (QMS, Pfeiffer-Balzer Omnistar) equipped with a 1 m long gas sampling capillary followed by an apertured entrance into the turbo-pumped QMS chamber.

Prior to data collection, as-synthesized $Au/LaPO_4$ was pretreated at 200 °C for 2 h in a flowing gas stream of either 2%O_2/He (O_2-pretreated) or 4%H_2/He (H_2-pretreated) and then cooled to rt in He. Then, a selected gas stream was introduced onto the sample with a total flow rate of 15 cm^3/min. The gas stream was either pure He, CO (2%CO/2%Ar/He) or a reaction mixture of CO and O_2 at a ratio of 1:4 (2%CO/2%Ar/He mixed with 2%O_2/He). In a typical switching experiment, two gas streams, flowing either through the DRIFTS cell or to a vent, were abruptly interchanged using a 4-way switching valve located upstream from the cell. The times described in the manuscript are relative to the time ($t = 0$) at which the inlet valve was switched. At the flow rate used, a delay time of about 20 s is required to reach the IR cell and about 40 s to reach the QMS. Alternatively, in a typical pulsing experiment, a six-way valve could be used to introduce a 0.5 cm^3 gas pulse into one of the gas streams. Both pulsing and switching experiments were carried out.

2.3. CO oxidation and temperature-programmed reduction

CO oxidation activity was tested in a plug-flow, temperature-controlled micro-reactor (Altamira AMI 200). For CO oxidation, the catalyst was loaded into a U-shaped quartz tube (4 mm i.d.) supported by quartz wool. The catalyst was pretreated online in flowing 2%O_2/He at 200 °C for 2 h and then cooled down before switching to the reaction mixture (36 cm^3/min mixture of 2%CO/2%Ar/He and 2%O_2/He). A portion of the product gas stream was extracted periodically with an automatic sampling valve and analyzed using a dual-column gas chromatograph with a thermal conductivity detector.

H_2 and CO temperature-programmed reduction (TPR) were also carried out in the AMI 200. Prior to TPR, each sample (50 mg) was first pretreated in 2%O_2/He gas mixture for 2 h at 200 °C. After being cooled down to rt, the sample was purged with high purity He (30 cm^3/min) for 15 min. Subsequently, a flow (30 cm^3/min) of 4%H_2/He or of 2%CO/2%Ar/He was switched into the system, and the sample was heated under this reducing gas flow from rt to 530 °C at a rate of 10 °C/min. In H_2-TPR, the consumption of H_2 was recorded using a TCD detector located downstream from a cold trap that removed H_2O. The TCD signal was calibrated by integrating pulses of 4%H_2/He from a calibrated loop sent through the TCD. In CO-TPR, the formation of CO_2 (and any H_2) was recorded using a downstream QMS. The QMS was calibrated by integrating pulses of CO_2 from a calibrated loop sent past the QMS sampling port.

3. Results

3.1. Temperature-programmed reduction in H_2

Previous work on $Au/FePO_4$ catalysts demonstrated that the $FePO_4$ support undergoes reduction during CO oxidation, contributing structural oxygen to the CO_2 product [28]. Since $LaPO_4$ is not expected to assume oxidation states lower than La^{3+}, it should not be able to contribute oxygen in this way. To verify this expectation, temperature-programmed reduction (TPR) was carried out for

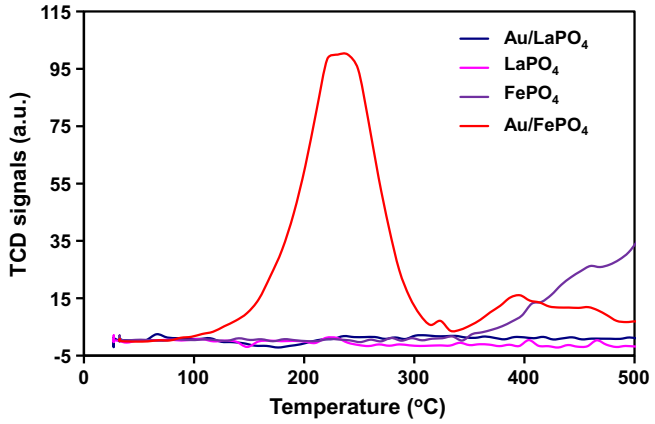

Fig. 1. H_2 temperature-programmed reaction is compared for both phosphate-supported Au catalysts and for the supports alone (without Au). Prior to TPR, the samples (approximately 50 mg) were first pretreated in 2% O_2/He gas mixture for 2 h.

Table 1
Product formation calculated from H_2-TPR.

Sample	H_2 consumed[a] (μmol H_2/g catalyst)	H_2 consumed[b] (mol H_2/mol Au)	H_2 consumed[b] (mol H_2/mol La or Fe)
$LaPO_4$	n/d	–	–
5.8 wt%Au/ $LaPO_4$	n/d	–	–
$FePO_4$	1050	–	0.166
2.5 wt% Au/ $FePO_4$	1833	14.4	0.283

[a] Integrated over TPR spectrum up to 500 °C.
[b] Calculated from col 2; n/d = not detected.

comparison of the reducibility of both Au/$LaPO_4$ and Au/$FePO_4$ catalysts as shown in Fig. 1. The results for Au/$FePO_4$ demonstrate significant H_2 uptake (reduction) in a prominent peak between 150 and 300 °C and a smaller amount of additional reduction above 400 °C. As pointed out previously [28], the $FePO_4$ in the absence of Au is much less reducible than the Au/$FePO_4$ catalyst under these TPR conditions, exhibiting one weak peak around 460 °C and further reduction that initiates above 500 °C. Thus, introduction of Au into $FePO_4$ accelerates the H_2 reduction of $FePO_4$, significantly lowering the H_2-TPR peak temperature. In marked contrast to the $FePO_4$-supported catalyst, there was no measureable reduction of either $LaPO_4$ or the $LaPO_4$-supported Au catalyst up to 500 °C.

Based upon calibrated measurement of the TCD response, the amount of H_2 consumed during TPR of the Au/$FePO_4$ was determined by integration of the TPD curves and the results are shown in Table 1, normalized to the mass of catalyst. Based upon the H_2 consumed and the Au loading, there is the equivalent of 10.5 μmoles of H_2/μmole Au in the peak at 250 °C and 14.4 μmoles of H_2/μmole Au including the reduction observed from 300 °C to 450 °C. Therefore, the amount of reduction far exceeds that needed for complete reductions of any Au^{III} to Au^0 and the H_2 consumption must correspond to the reduction of $FePO_4$ which is reducible to $Fe_2P_2O_4$ or to $Fe_3(P_2O_7)_2$ depending upon the P/Fe ratio [29]. In fact, the amount of H_2 consumed was sufficient to reduce all of the Au and a substantial portion (50–56%) of the Fe^{III} to Fe^{II}. The main conclusion is that H_2 pretreatment of Au/$FePO_4$ at 200 °C leads to substantial (but still incomplete) reduction of the catalyst, while no reduction by H_2 of the Au/$LaPO_4$ is expected.

3.2. CO adsorption and desorption with different treatments

Interactions of CO with the catalysts were studied by monitoring adsorption and desorption of CO during transient gas switches. Initially, the pretreated sample was exposed to 2%CO for an extended period (5–30 min) at rt to saturate the surface. Fig. 2 shows the evolution of the IR spectra from O_2-pretreated Au/$LaPO_4$ when the 2%CO/2%Ar/He stream is switched to He (Fig. 2a) or switched to 2%O_2/He (Fig. 2b). During the CO saturation, the spectrum is dominated by a broad CO stretching band near 2102 cm^{-1}, a sharp adsorbed CO_2 peak at 2345 cm^{-1} and a broad peak at 2164 cm^{-1} (dashed spectrum in Fig. 2a). The band at 2102 cm^{-1} is assigned to CO adsorbed on metallic Au (Au^0) based on previous work [28]. The band at 2164 cm^{-1} is at the correct position and has the shape that suggests that it is due to gas-phase CO in the DRIFTS cell. Upon switching to He, it disappears at a rate comparable to the rate of decrease in the Ar marker (as measured by the QMS). The adsorbed CO_2 peak at 2345 cm^{-1} seen during CO adsorption is unexpected and is accompanied by a variety of bands in the carbonate region (Supplementary material, Fig. S1). The CO_2 peak grows in quickly upon introducing CO, saturates after about 5 min and then gradually decreases with continued CO exposure. It is indicative of CO_2 formation and its weak adsorption on the catalyst. Similar experiments were also performed on Au-free $LaPO_4$ pretreated under similar conditions, and it exhibited no CO features in the linear stretching region although there was indication of formation of carbonates.

During desorption in He (Fig. 2a), the adsorbed CO band changes shape as it decreases in intensity. An unusual red-shifted, broad adsorption band becomes apparent, first peaking at 2075 cm^{-1} and then shifting to 2050 cm^{-1}. IR bands in this region for CO adsorption on Au/ TiO_2, Au/ Fe_2O_3 and Au/CeO_2 catalysts have been reported previously by Boccuzzi et al. [30–32]. These authors assigned these bands to adsorption on small clusters of negatively charged Au that result from electron transfer from the reduced support. However, it is worthwhile to stress that IR bands due to adsorbed CO in the 2075–2050 cm^{-1} spectral range have never been detected on supported gold catalysts without pre-reduction. In the present case, these bands at 2075–2050 cm^{-1} are observed at rt on the Au/$LaPO_4$ catalyst that was O_2-pretreated. Interestingly, these low-frequency bands are not apparent during the CO adsorption process except as a slight broadening on the low-frequency side of the 2102 cm^{-1} peak (see Fig. S1). It is likely that the component at 2075 cm^{-1} is present but hidden under the strong band at 2102 cm^{-1} after the saturation in CO.

The gradual shift from 2075 to 2050 cm^{-1} upon desorption is attributed to the decrease in dipole–dipole coupling between adsorbed CO molecules as coverage decreases. The observation of the 2075 and 2050 cm^{-1} band due to CO on negatively charged Au (anionic Au) can be taken as an indication of a chemical change involving charge transfer that occurs during long exposure to CO, i.e. CO changes the surface of the Au/$LaPO_4$ catalyst during the rt adsorption process. A chemical change is already indicated by the simultaneous evolution of CO_2 and formation of carbonates (Fig. S1) during the CO adsorption stage. The data indicate that CO reacts with oxygen-containing species on the surface of Au/$LaPO_4$ catalyst, producing CO_2 and carbonates and creating negatively charged Au.

If instead of desorbing the CO in He, the CO–saturated surface is exposed to O_2, different behavior is observed (Fig. 2b). As expected, gas-phase CO_2 due to reaction of O_2 with adsorbed CO occurs and so the surface CO is removed faster than during desorption. During this exposure, the band at 2102 cm^{-1} decreases and blue shifts to 2128 cm^{-1}. On the basis of previous work [28,33], the 2128 cm^{-1} band can be assigned to CO adsorbed on gold particles that are to some extent made electropositive by adsorbed oxygen. Unlike the case of desorption in He, bands at 2075 cm^{-1} and 2050 cm^{-1} are not clearly observed. Evidently, by interaction with O_2 at rt, the negative charge on Au is transferred to the site on which oxygen is adsorbed. Another explanation is that CO adsorbed on the

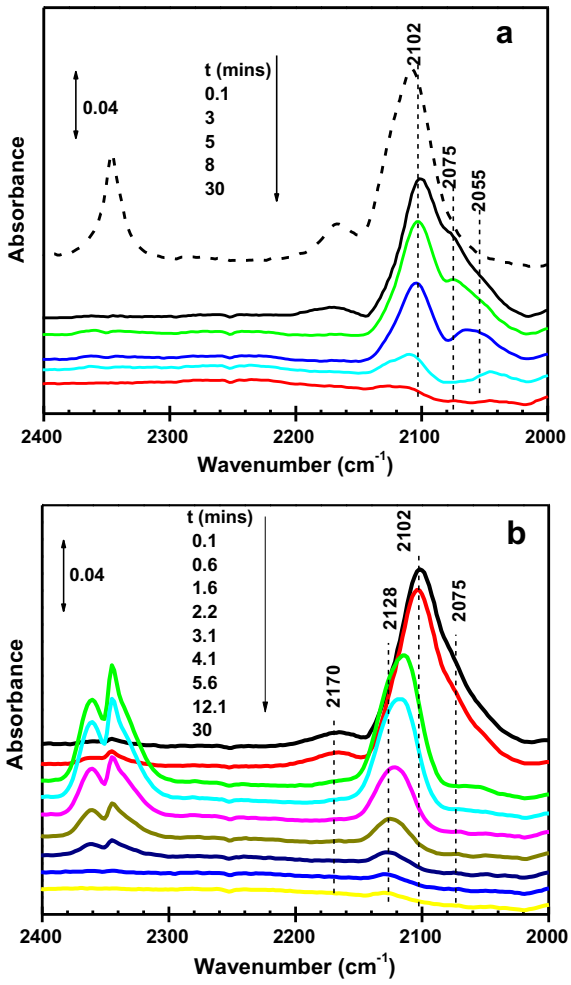

Fig. 2. Time evolution of the FTIR of the CO stretching region is shown for the O_2-pretreated $Au/LaPO_4$ catalyst during CO desorption. *Upper panel.* Dashed line shows spectrum after saturation CO exposure. Solid curves show the time evolution after a gas switch from 2%CO/2%Ar/He to He. *Lower panel.* Solid curves show the time evolution after a gas switch from 2%CO/2%Ar/He to 2%O_2/He.

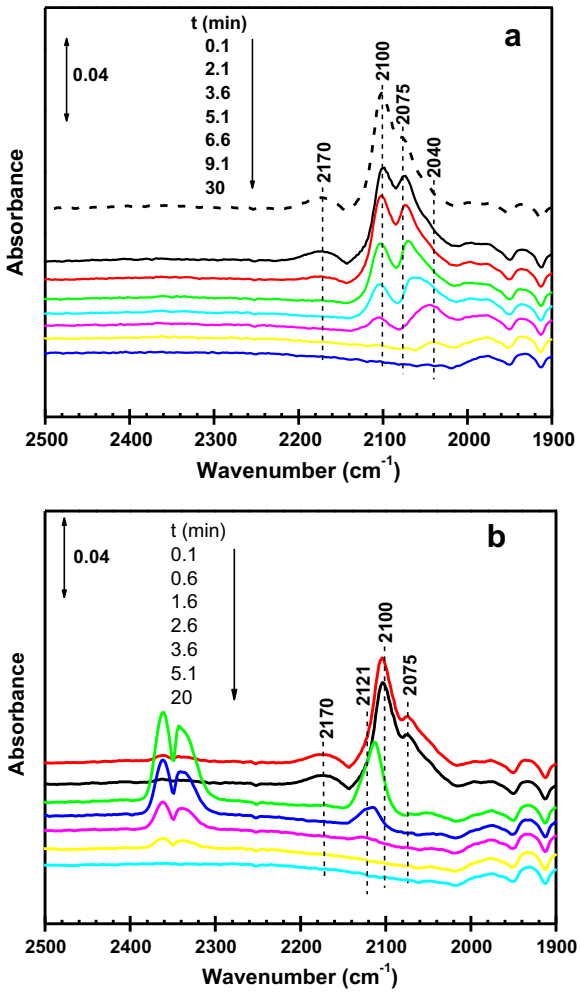

Fig. 3. Time evolution of the FTIR of the CO stretching region is shown for the H_2-pretreated $Au/LaPO_4$ catalyst during CO desorption. *Upper panel.* Dashed line shows spectrum after saturation CO exposure. Solid curves show the time evolution after a gas switch from 2%CO/2%Ar/He to He. *Lower panel.* Solid curves show the time evolution after a gas switch from 2%CO/2%Ar/He to 2%O_2/He.

negatively charged gold particles is more reactive to oxygen than that on metallic gold particles.

Analogous CO adsorption and desorption/reaction experiments were also carried out on a H_2-pretreated sample as shown in Fig. 3. Flowing CO at rt onto pre-reduced $Au/LaPO_4$ sample (Fig. 3a dashed curve) gives the main band at 2100 cm^{-1} due to CO adsorption on the metallic Au. Unlike the case of the O_2-pretreated catalyst, no CO_2 adsorbed peak is ever observed during the CO adsorption, and the band at 2075 cm^{-1}, assigned to CO adsorption on negatively charged Au, is more apparent after CO adsorption and during subsequent desorption. These differences indicate that the surface of $Au/LaPO_4$ sample is changed during H_2 treatment. During desorption in He, the band at 2070 cm^{-1} is relatively intense and decreases more slowly than the band at 2100 cm^{-1}. Thus, it appears that the CO associated with the negatively charged Au may be more strongly bonded and slower to desorb than the CO adsorbed on metallic Au^0 as has been observed previously [30]. During desorption/reaction in O_2 (Fig. 3b), the IR spectra show similar trend as on the O_2-pretreated sample.

Gas switching results given in Figs. 2 and 3 for $Au/LaPO_4$ are summarized in Fig. 4 and compared with results from similar experiments performed on $Au/FePO_4$. The integrated intensity of the manifold of CO stretching features is shown as a function of time for the two types of gas switches (CO to He and CO to O_2) and for the two different pretreatments (O_2 and H_2 pretreatments). In each case, the downstream Ar QMS signal intensity is given as a reference that describes the rate at which gas is removed from the DRIFTS cell. For the $LaPO_4$-supported Au catalyst, the CO decrease is nearly independent of whether the sample is H_2- or O_2-pretreated, consistent with the fact that both treatments give the same Au oxidation states. The decrease is more rapid in O_2/He than in He demonstrating that CO oxidation reaction occurs at rt. Loss of CO by reaction with O_2 is about as fast as the loss of Ar signal indicating that the oxidation is rapid compared to the rate of gas removal from the DRIFTS. For the $Au/FePO_4$ sample, there is a more pronounced difference between H_2-pretreated and the O_2-pretreated catalyst during both desorption in He and desorption/reaction in O_2/He. As reported previously, on $FePO_4$, the oxidative treatment leads to cationic Au that bonds CO in a state that is more tightly bound and less reactive toward O_2.

3.3. CO_2 formation and reduction properties of phosphates

The formation of CO_2 during CO adsorption on $Au/LaPO_4$ indicates that there is active oxygen available on the catalyst surface after O_2 pretreatment. FTIR results indicate that gold is observed to be metallic or negatively charged (Fig. 2a), and therefore, it is

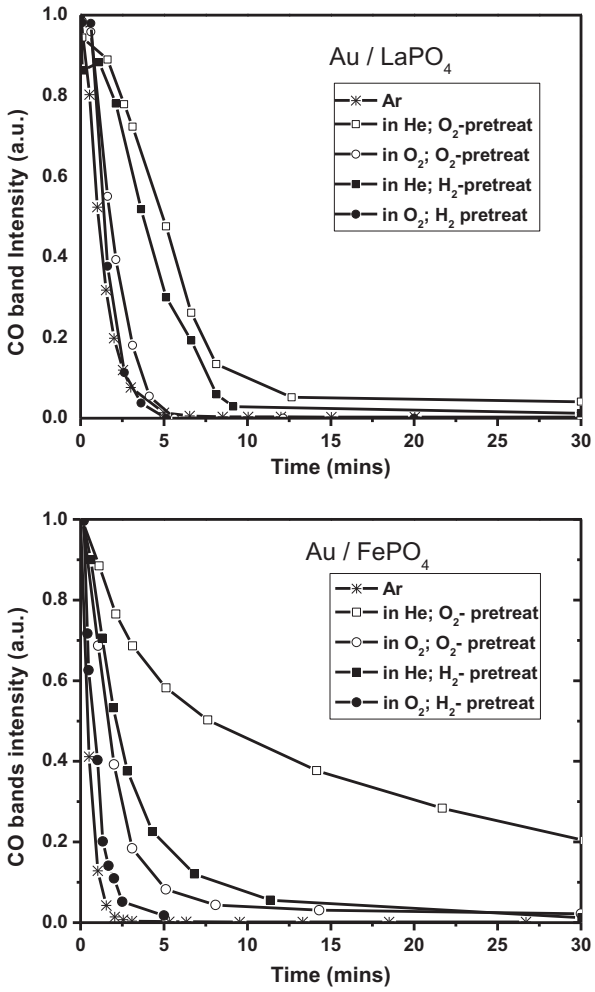

Fig. 4. *Upper panel*: The rate of decrease in adsorbed CO from $Au/LaPO_4$ during rt desorption into He or during rt desorption/reaction into O_2 is shown for both the H_2-pretreated and the O_2-pretreated. The flow rate is 15 ml/min. Downstream measurement of the Ar QMS intensity is shown for reference and is offset in time by the delay required for the gas to reach the QMS sampling port. *Lower panel*: Same as upper panel except for $Au/FePO_4$.

not present as an oxide Thus, reduction of Au oxide is not responsible for the CO_2 formation. We conclude that the active oxygen species on $Au/LaPO_4$ that is consumed to evolve CO_2 at rt must be from either chemisorbed oxygen or structural oxygen from $LaPO_4$. However, it is unexpected that rt CO can remove structural oxygen from $LaPO_4$ because $LaPO_4$ is generally considered to be non-reducible.

To clarify the source of active oxygen in $Au/LaPO_4$, isotopic IR experiments were carried out as shown in Fig. 5. First, $Au/LaPO_4$ was pretreated for 1 h at 200 °C in $^{18}O_2$ and then cooled in $^{18}O_2$ followed by purging with He at rt. Next, He was switched to $C^{16}O$ while monitoring FTIR and downstream QMS. This switch to $C^{16}O$ resulted in the production of $C^{16}O^{18}O$, suggesting the existence of either chemisorbed $^{18}O_2$, formation of peroxides or incorporation of ^{18}O into the $Au/LaPO_4$ during the pretreatment in $^{18}O_2$. Raman experiments were also conducted to clarify the source of oxygen. Previously, we demonstrated that for $Au/FePO_4$ treatment with CO at rt leads to a change in the Raman spectrum that is consistent with the removal of oxygen and reduction of the $FePO_4$ [28]. Similar experiments during rt CO exposure of O_2-pretreated $Au/LaPO_4$ showed no changes in the Raman spectrum, consistent with no structural change of the $Au/LaPO_4$ sample (Fig. S2). Therefore, we speculate that the active oxygen species responsible for the evolution of CO_2 must originate from chemisorbed oxygen or hydroxyl groups on the $Au/LaPO_4$.

To further characterize the availability of active oxygen, we performed CO-TPR experiments for both the Fe and La phosphate-supported catalysts and these are presented in Fig. 6. The TPR profile of $FePO_4$ sample without Au exhibited one weak CO_2 formation peak with a maximum at 350 °C together with incomplete additional reduction initiated just below 500 °C. The $FePO_4$ with 2.5 wt% Au loading showed an intense CO_2 formation peak around 230 °C and less pronounced reduction features peaking near 90 °C, 400 °C and 480 °C. The amount of CO_2 formed during the TPR was quantified by comparison with pulses of CO_2 and the results are provided in Table 2. The amount of CO_2 formed was found to be about 0.61 mol CO_2 per mole of $FePO_4$. As expected from reactions,

$$3CO + Au_2O_3 \rightarrow 3CO_2 + 2Au^0 \quad (1)$$

$$CO + 2Fe^{III}PO_4 \rightarrow CO_2 + Fe^{II}_2P_2O_7 \quad (2)$$

the complete reduction of Fe^{III} to Fe^{II} and of all Au from Au^{III} to Au^0 would lead to 0.525 mol of CO_2 formed per mole of Fe in the 2.5 wt% $Au/FePO_4$ catalyst. It is obvious that the CO_2 formation observed in $Au/FePO_4$ CO-TPR profile is sufficient to imply complete reduction of not only the Au but also all of the $FePO_4$. Thus, when compared to H_2, CO is a stronger reductant for the reduction of $FePO_4$ with Au assistance. This is in agreement with our previous report that CO can react with structural active oxygen of $FePO_4$ even at rt with help from Au. It is evident that the presence of gold enhances the reduction of Fe^{III} by both H_2 and CO. The absence of H_2 during CO-TPR suggests that the reduction of (surface) hydroxyl groups is negligible for both $FePO_4$ and $Au/FePO_4$.

CO-TPR profiles for $LaPO_4$ and $Au/LaPO_4$ are shown for comparison in Fig. 6a and b. The $LaPO_4$ exhibits one weak CO_2 formation peak at a relatively low temperature near 70 °C. Considering the difficulty of reducing $LaPO_4$, this weak CO_2 peak most likely arises from a form of surface oxygen chemisorbed during the O_2 pretreatment process. The amount of CO_2 formed on the basis of quantitative calculations with this peak was 0.016 mol CO_2/mol La (Table 2). After the introduction of gold onto $LaPO_4$, more CO_2 formation was observed in CO-TPR, 0.10 mol CO_2/mole La, with a peak maximum at 168 °C. This ratio suggests that the consumption of O by CO is confined to a limited region, probably the surface region of the $LaPO_4$. Since the gold is present as metallic and negatively

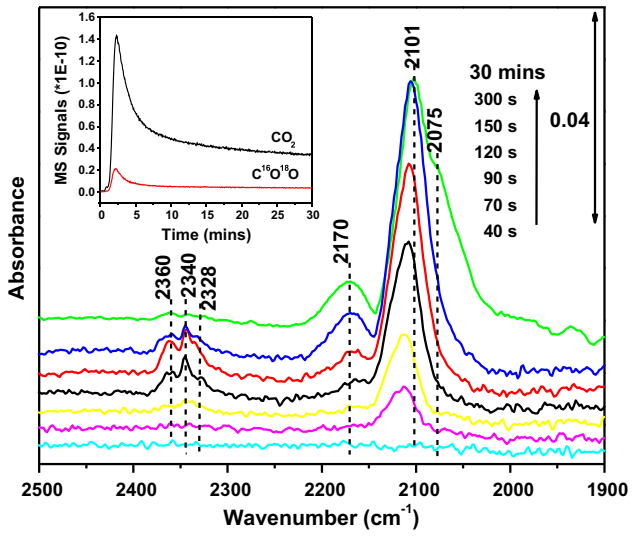

Fig. 5. IR spectra and QMS (inset) results for CO adsorption at rt on $^{18}O_2$-pretreated $Au/LaPO_4$ as a function of adsorption time after switching from He to CO.

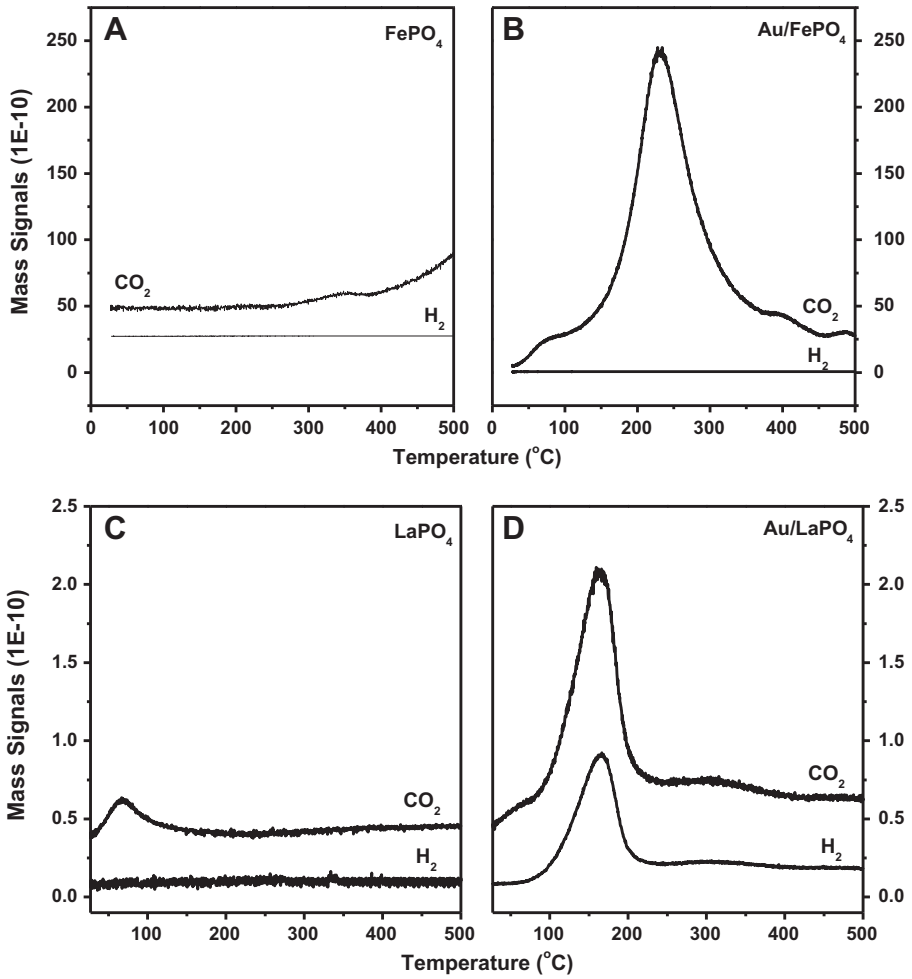

Fig. 6. CO temperature-programmed reaction is compared for $FePO_4$ (A), $Au/FePO_4$ (B) and the $LaPO_4$ (C), $Au/LaPO_4$ (D). The H_2 signal is scaled according to the CO_2:H_2 QMS sensitivity ratio.

Table 2
Product formation calculated from CO-TPR.

Sample	CO_2 formed[a] (μmol/g catalyst)	CO_2 formed[b] (mol CO_2/mol La or Fe)	H_2 formed[a] (μmol/g catalyst)	H_2 formed[b] (mol/mol La or Fe)
$LaPO_4$	68	0.016	n/d	–
5.8 wt%$Au/LaPO_4$	423	0.10	214	0.053
$FePO_4$	468	0.07	n/d	–
2.5 wt% $Au/FePO_4$	3960	0.61	n/d	–

[a] Integrated TPR spectrum up to 500 °C.
[b] Calculated from preceding col; n/d = not detected.

charged Au after O_2 pretreatment (Fig. 2), then reduction of Au oxide cannot be the source of CO_2. The observation of H_2 formation peak at the same temperature as the CO_2 formation suggests instead that the reaction involves attack of hydroxyl groups by CO according to reaction 3 or 4.

$$CO + OH^- \rightarrow CO_2 + 1/2H_2 + \square^{1-} \quad (3)$$

$$CO + 2OH^- \rightarrow CO_2 + H_2 + O^{2-} \quad (4)$$

The observed amount of H_2 produced is very close to half of the CO_2 produced (Table 2) consistent with reaction according to reaction (3). The results indicate that surface hydroxyl on $LaPO_4$ is reactive toward CO adsorbed on Au nanoparticles, yielding CO_2 and H_2 and leaving a hydroxyl vacancy site, $\square^{1-}$, on $LaPO_4$. This loss of oxygen (hydroxyl) from the phosphate anion may be related to the formation of negatively charged Au state shown in Fig. 1. Because the evolution of H_2 was not observed over $LaPO_4$ alone during CO-TPR, the presence of Au species must enhance the removal of the hydroxyl group from $Au/LaPO_4$ sample. It is reasonable that only hydroxyl groups adjacent to Au species could be attacked by the CO. The absence of reaction of CO with hydroxyls on the $Au/FePO_4$ is consistent with the absence of anionic Au on the $Au/FePO_4$

Reaction (4) is not consistent with the results since only half of the CO_2 formation observed in Fig. 6d could arise from this reaction. The remainder of the CO_2 formation must come from CO reaction with surface structural oxygen of $LaPO_4$ and leading to the structural change of $LaPO_4$ support surface. However, there is no structural change observed in the Raman results as we stated earlier. These two results therefore confirm that reaction (3) is the applicable pathway. These observations combined with the quantitative results of CO-TPR for $LaPO_4$ sample reveal that the origin of the CO_2 evolution observed during CO chemisorption (Fig. 1) is

reaction with surface hydroxyl groups, through formation of carbonates or bicarbonate intermediates, and this is possible even though the $LaPO_4$ is fundamentally non-reducible material.

To clarify whether this removed hydroxyl group can be replenished, repeated CO-TPR were performed on the O_2-pretreated Au/$LaPO_4$. After the first CO-TPR with temperature up to 500 °C, the sample was subjected to an intermediate O_2 flow at rt and then to He purging before performing another CO-TPR. This second CO-TPR (not shown) gave an almost identical profile (the position and relative intensity of H_2 and CO_2 peaks) to the first one. Therefore, it appears that the active hydroxyl groups that are consumed to evolve CO_2 as shown in Fig. 6d are readily replenished by the low concentration of H_2O present in the O_2 and/or He gas steams used in these experiment. Since O_2 is also expected to react quickly with the hydroxyl defects, it seems that the water must compete with, displace or protonate the oxygen on the Au/$LaPO_4$ surface.

3.4. Activity measurement

In our previous study, to determine the role of the redox property of Au/$FePO_4$ and the state of Au species during continuous CO oxidation reaction, $^{16}O_2$-treated Au/$FePO_4$ was used to catalyze CO oxidation by labeled $^{18}O_2$ at rt [28]. The results of CO oxidation with labeled $^{18}O_2$ suggest the operation of two parallel reaction pathways at rt: (1) a redox pathway in which $FePO_4$ supplies active oxygen and (2) a direct pathway on metallic Au, in which gas-phase O_2 provides the active oxygen.

For comparison, the same experiment was carried out here for Au/$LaPO_4$ pretreated in O_2/He as shown in Fig. 7. Three bands at 2360, 2340 and 2325 cm^{-1} assigned to gaseous $C^{16}O_2$ and $C^{16}O^{18}O$, appear immediately after introducing the CO and $^{18}O_2$ reaction mixture. The unlabeled CO_2 at 2360 and 2340 cm^{-1} may derive from the reaction between CO and chemisorbed oxygen and /or active hydroxyl group on Au/$LaPO_4$ catalyst. The $C^{16}O^{18}O$ is produced from the Au-catalyzed reaction between CO and the incoming $^{18}O_2$. As the reaction continues, the intensity of the gas-phase $C^{16}O_2$ band at 2360 cm^{-1} decreases with time on stream due to the limited ^{16}O source on the surface. Metallic Au is initially present after pre-oxidation treatment as indicated from Fig. 2. The immediate appearance of $C^{16}O^{18}O$ confirms the positive role of this metallic Au in catalyzing CO oxidation at rt on phosphates-supported Au catalysts. Simultaneous appearances of $C^{16}O^{18}O$ and $C^{16}O_2$ indicate that CO reaction with gas-phase O_2 and CO reaction with adsorbed hydroxyl group initiate at the same time upon introduction of CO oxidation conditions. This last result differs slightly from the case for Au/$FePO_4$. For Au/$FePO_4$, the appearance of $C^{16}O^{18}O$ is delayed relative to $C^{16}O_2$ and its parallel growth with the CO–Au^0 band (2114 cm^{-1}) suggests that the production of $C^{16}O^{18}O$ takes place only after metallic Au is formed from the reduction of cationic Au by CO. As concluded previously, cationic Au present on O_2-pretreated Au$FePO_4$ is less active and becomes more active after it is reduced to the metallic state.

Upon introduction of reaction conditions, the CO peak position initially appears and persists near 2115 cm^{-1}, as shown in Fig. 7. Although the metallic and anionic Au obtained on the oxidatively treated Au/$LaPO_4$ sample exhibit two CO peaks at 2102 and 2070 cm^{-1} during CO adsorption and desorption (Fig. 2), these positions are altered by O_2 in the reaction stream. The lack of a band for CO adsorbed on negatively charged Au (at 2070 cm^{-1}) under reaction conditions in Fig. 7 suggests the negative charge is transferred to the catalyst surface when oxygen is adsorbed. The shift of the metallic band from 2102 to 2115 cm^{-1} is not attributed to any change in the oxidation state of the Au since the shift is quite small and the frequencies are in the right range for adsorbed CO on metallic Au [34]. It is attributed to the presence of O_2-like species adsorbed on the Au. Such an effect of O_2 was reported for

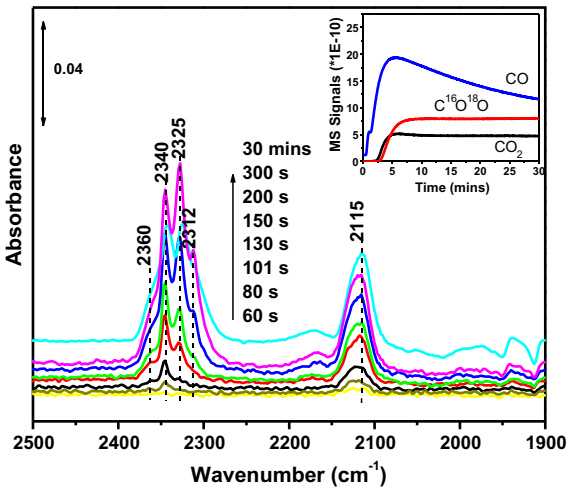

Fig. 7. IR spectra and QMS (inset) results following switch from He to CO + $^{18}O_2$ at rt as a function of time after the switch. The Au/$LaPO_4$ catalyst was pretreated in $16O_2$ at 200 °C.

Au/SiO_2 [33], and an identical blue shift was observed for the H_2-pretreated Au/$FePO_4$ that contains only metallic Au.

The catalytic performance of Au/$LaPO_4$ and Au/$FePO_4$ was also investigated in a micro-reactor system. The activity results are compared in Table 3 where the specific reaction rates are extracted from the conversion at two different temperatures and normalized to the total Au loadings. For Au/$LaPO_4$, both oxidative and reductive treatments give similar CO conversion and turnover frequency (TOF). This is clearly correlated to the similar Au species (metallic and anionic Au) present over $LaPO_4$, after the two different types of treatment (as indicated by IR data in Figs. 2 and 3). However, the reductively pretreated Au/$FePO_4$ catalyst exhibited higher rates of CO_2 formation at the temperature investigated, approximately twice that of the oxidatively treated Au/$FePO_4$ catalyst. This again shows that the metallic Au species plays a major role in CO oxidation on Au/$FePO_4$ at rt, whereas the cationic Au species is inactive or only weakly active. Compared with Au/$FePO_4$, the CO conversion and turnover frequency (TOF) are higher on Au/$LaPO_4$ catalyst.

4. Discussion

CO_2 is produced upon exposing the O_2-pretreated samples of either Au/$FePO_4$ or Au/$LaPO_4$ to CO at rt (compare Li et al. [28] and Fig. 2). This transient CO_2 evolution indicates that active oxygen species is available on both of Au/$FePO_4$ and Au/$LaPO_4$ sample. For Au/$FePO_4$ sample, we previously demonstrated that the active oxygen species leading to CO_2 evolution originates from both the reduction of cationic Au and capture of structural oxygen from the $FePO_4$ support in the O_2-pretreated sample. It was also demonstrated that the structural active oxygen species in the $FePO_4$ that is consumed to evolve CO_2 can be replenished by gas-phase O_2 at rt in the present of Au species.

Since $LaPO_4$ is expected to be non-reducible, it is of interest to consider how CO_2 can be produced by exposure to CO at rt. The present H_2-TPR and CO-TPR studies provide important clues to explain this point. As described above, significant differences were observed between H_2-TPR and CO-TPR for Au/$LaPO_4$ and $LaPO_4$ samples. The H_2-TPR (Fig. 1) shows no detectable indication of reduction of either $LaPO_4$ or Au/$LaPO_4$ samples up to 500 °C as would be expected. But the CO-TPR profile of $LaPO_4$ shows one weak CO_2 formation peak with a maximum around 70 °C, while the profile for Au/ $LaPO_4$ shows in addition a more intense CO_2 formation peak near 170 °C (Fig. 6d). This higher temperature peak was accompanied by the formation of H_2. From the amount of CO consumed in the low- and the

Table 3
Activity for CO oxidation.[a]

Catalysts	Au density[b] (Au atoms/ nm^2)	Rate at 0 °C[c] (mol CO/ (mol Au s))	Rate at 23 °C[c] (mol CO/ (mol Au s))
5.8 wt% $Au/LaPO_4$ oxidative treatment	3.2	0.035	0.042
5.8 wt% $Au/LaPO_4$ reductive treatment	3.2	0.028	0.038
2.5 wt% $Au/FePO_4$ oxidative treatment	2.8	0.0079	0.015
2.5 wt% $Au/FePO_4$ reductive treatment	2.8	0.018	0.031

[a] Reaction conditions: 1%CO/1%O_2/He, flow rate = 36 ml/min; W/F adjusted to give conversions <60%.
[b] Based upon $LaPO_4$ surface area = 56 m^2/g; $FePO_4$ surface area = 27.5 m^2/g.
[c] Normalized to total Au, Au wt loadings determined by X-ray fluorescence.

high-temperature peaks, we suggest that the low-temperature CO_2 formation peak could be from the reaction of CO with some form of chemisorbed oxygen, which is adsorbed with or without Au being present. We propose that the high-temperature peak involves the reaction between a surface hydroxyl group and CO to create CO_2 and a surface hydroxyl "vacancy," as described by reaction (4). Such a reaction must be catalyzed by the Au species near the hydroxyl groups since there is no H_2 formation observed on the $LaPO_4$ alone. Evidently, water reacts rapidly with the CO reduced surface to re-create the surface hydroxyl since flowing gas-phase O_2 at rt (presumably with a low concentration of adventitious H_2O impurity) reestablishes their presence.

Numerous studies have reported that the reduction temperature of metal oxides by H_2 can be lowered by the addition of transition metals with Pt and Pd being the most efficient metals [35] but the effect has also been for Au particles supported on CeO_2(1 1 1) [36]. In particular, enhanced reduction of Fe_2O_3 and of $FePO_4$ by H_2 has been reported in Pt/Fe_2O_3 and $Rh/FePO_4$ catalysts [37,38]. We report here that the presence of gold accelerates the H_2 reduction of $FePO_4$ as indicated by significantly lowered H_2-TPR peak temperature (Fig. 1). It can be assumed that H atoms generated by the dissociative chemisorption of H_2 on the reduced Au^0 migrate onto the $FePO_4$ to enhance reduction of surface phosphate. The amount of H_2 consumed is so large (Table 1) that a substantial fraction of the bulk $FePO_4$ must be reduced. Evidently, the reduction of Au-free $FePO_4$ is rate limited by the dissociation of H_2, but it can be assumed that the reduction occurs facilely in the presence of adsorbed H atoms. Reduction of $LaPO_4$ by H_2 does not occur (Fig. 1) even when reduced Au is present to create H atoms and hydroxyls species, and the reason is the non-reducibility of the La^{3+} cations.

We also find that Au enhances the reduction of $FePO_4$ (Fig. 6b) by CO. Enhanced CO reduction has been reported in reducible oxides used for oxygen storage in emission catalysts. For example, Deganello et al. [39] recently reported that the reduction peak of CeO_2 or $Ce_{0.6}Zr_{0.4}O_2$ shifts to a significantly lower temperature by addition of Pt deposition, and they have suggested that the Pt facilitates the release of CO_2. Our data show that CO adsorbed on Au^0 or Au^I reacts with oxygen from the support, possibly by backspillover of oxygen from nearby regions of the $FePO_4$. Loss of oxygen occurs with reduction of Fe^{3+} to Fe^{2+} as suggested by Raman spectroscopy [28] to form a reduced phosphate such as $Fe_2P_2O_7$. Such reduction has been noted previously for $FePO_4$ catalyst when exposed to reductive conditions [40]. As with the H_2, CO is able to reduce a substantial fraction of the $FePO_4$. The reduction of the $FePO_4$ is accompanied by reduction of the Au, a portion of which is still present in cationic form after the O_2 pretreatments as described previously [28]. In the $Au/LaPO_4$ case, more than six times less CO_2 is evolved compared to the $Au/FePO_4$ catalysts (Table 2). This is approximately consistent with the extent of CO_2 formation by the $Au/LaPO_4$ being limited to removal of surface hydroxyls. CO clearly reacts strongly with the surface of $Au/LaPO_4$ catalyst (either with chemisorbed oxygen or hydroxyl groups) as indicated by the FTIR spectrum (Fig. 2). Exposure of the O_2-pretreated surface to CO produces adsorbed CO_2 and a manifold of peaks in the range of 1300–1450 cm^{-1} and 1600–1700 cm^{-1} that we associate with growth of carbonates, bi-carbonates and formate (Fig. S1). These processes are presumed to be limited to the surface of the catalyst, especially the $LaPO_4$ support, and related to the evolution of gas-phase H_2 and CO_2 observed in the CO-TPR.

For $Au/LaPO_4$ sample, the present results show that metallic and anionic Au are present after both oxidative and reductive treatment. The bands of CO adsorbed on the anionic Au are present at 2075–2050 cm^{-1}. A band in 2000–2075 cm^{-1} spectral range has been reported by Menegazzo et al. [32] for Au on a reducible support. CO adsorption gives rise to a broad band in this region for Au supported on CeO_2 following reduction at 100 °C and deliberate exposure to water at rt. They attributed this band to CO adsorbed on small clusters of negatively charged Au that result from electron transfer from the reduced support. In electrochemical studies of gold electrodes during the electro-oxidation of CO, a low-frequency CO adsorption band (1920–1970 cm^{-1}) has been observed that is strongly potential dependent [41,42]. Its strongly red-shifted position has been attributed to back bonding to the CO $2\pi*$ orbital and possibly related to OH^- ions [42]. In our case, this negatively charged Au is caused probably by an excess in negative charge transferred from the support that results from the changes caused by interaction between the CO and the $LaPO_4$. We propose that in this case, it is primarily the loss of the hydroxyl and the interaction of the Au at the resulting site that leads to the negatively charged Au. Anionic Au has not been detected on oxide-supported catalysts unless the oxide is reducible and has been pre-reduced [32], while for the $Au/LaPO_4$, we observe anionic Au on non-reducible $LaPO_4$ after the O_2 pretreatment. Similarly, Park et al. saw anionic Au form on $AlPO_4$, another non-reducible support [43]. Evidently, a reducible support is not a requirement for creation of anionic Au. For comparison, as we reported in our previous work [28], the different treatments of $Au/FePO_4$ lead to as many as four different CO adsorption frequencies, each signaling a different Au adsorption environment. Cationic Au is present after oxidative treatment, and metallic Au dominates after reductive treatment. The majority of this cationic Au undergoes *in situ* reduction to metallic Au during rt CO adsorption. Interestingly, anionic Au is not seen on the reducible $Au/FePO_4$ catalyst, even after reductive treatment. Evidently, a reducible support is not a sufficient condition for creation of anionic Au. We propose that it is changes related to surface oxygen and hydroxyl that determine the conditions necessary for creation of anionic Au.

Information about the reactivity of CO adsorbed on the sites characterized by different Au oxidation states can be obtained from contrasting the loss of CO from the surface by desorption (in He) compared to reaction with O_2. The plots of the IR band (CO on gold) intensity change as a function of time are shown in Fig. 4 for the two cases and for both catalysts. In the case of $Au/FePO_4$, the IR band due to adsorbed CO on the metallic Au (H_2-pretreated) decreased much more rapidly than that on the mixture of cationic and metallic Au (O_2-pretreated). This information clearly indicates that metallic Au plays a major role in CO oxidation on $Au/FePO_4$ at rt, whereas the cationic Au species alone is weakly or not active. Similarly, the CO decreased much faster in O_2 than in He for $Au/LaPO_4$ that has both metallic and anionic Au resulting from either oxidative or reductive treatments (Fig. 4) and the CO reacts in O_2

rapidly from both the metallic and anionic Au. This information indicates that metallic Au is active in this case also. The CO adsorbed on negatively charged Au on the $LaPO_4$ is unstable in the O_2 atmosphere as shown in Figs. 2 and 3. The loss of CO adsorbed on negatively charged Au could happen for either of two reasons: (1) CO adsorbed on the negatively charged gold particles is reactive and is removed by reaction with O_2 or (2) interaction with O_2 at rt causes the negative charge on the Au to be transferred to the surface of catalyst where oxygen is adsorbed.

The above information on the nature of surface Au sites and reducibility of $FePO_4$ and $LaPO_4$ is critical for revealing the reaction mechanism of CO oxidation, including the catalytically active Au sites and the reaction pathways. In our previous work, CO oxidation results demonstrate that CO can be oxidized by structural O of $FePO_4$ and that O_2 can be activated by the thusly reduced support. Isotope studies using $^{18}O_2$ demonstrate that the redox pathway occurs in competition with the direct reaction catalyzed by metallic Au. On the basis of the results presented in this work, we find that chemisorbed hydroxyls, ubiquitous on the $LaPO_4$ surface under typical reaction conditions, can also react to oxidize CO catalyzed by the Au. This reaction pathway has been previously suggested for other non-reducible oxides, such as SiO_2. For Pt supported on mesoporous SiO_2, Fukuoka et al. [44] have demonstrated the incorporation of support-oxygen into the product CO_2 by the IR experiments using the isotopic tracer technique. From the experimental results, they conclude that the CO oxidation is promoted by the attack of OH groups at the internal surface of mesoporous silica toward CO on Pt. Costello et al. [19,20] have shown that the presence of hydroxyls, as introduced by exposure to H_2 or H_2O, has a large positive effect upon the activity of Au/Al_2O_3. They propose that reaction between CO and OH to form a hydroxy carbonyl on the Au clusters is the primary reaction pathway for CO oxidation. In the present case of $Au/LaPO_4$, it is apparent that surface hydroxyls, assumed to be initially present on the $LaPO_4$ support, can react with CO to form CO_2. In the case of $Au/FePO_4$, structural oxygen from the support can also contribute to the CO oxidation.

Although our FTIR results suggest two different pathways in which the support contributes to CO oxidation, our reactivity measurements suggest that these reaction pathways are not the primary pathways, as long as small particle, reduced Au is present. The catalytic performance (Table 3) results show that the H_2-pretreated $Au/FePO_4$ catalyst exhibits higher rates of CO_2 formation than the O_2-pretreated $Au/FePO_4$ at the temperatures investigated. After reductive treatment, there is less available structural oxygen on the $FePO_4$ but there are more available reduced Au sites. We conclude that it is the reduced Au, not the availability of reducible support, that is critical. Similarly, in spite of not having available structural oxygen, $Au/LaPO_4$ catalyst gave higher CO conversion and turnover frequency (TOF) than the $Au/FePO_4$ catalyst, for both oxidative and reductive treatments. The information points out that metallic Au is active site for CO oxidation over phosphates-supported Au catalysts. Based upon these results, it is obvious that support reducibility does not guarantee high activity. The results for both $Au/LaPO_4$ and $Au/FePO_4$ suggest that neutral Au is more active than cationic Au, although it is yet possible to compare the activity of the negatively charged Au apparent on the $LaPO_4$ surface. Also, our results cannot differentiate whether the "direct" pathway, i.e. reaction of dissociatively adsorbed O_2 with CO on the Au particles, is mediated by OH.

5. Conclusion

We have presented a direct comparison between a reducible and non-reducible phosphate support used to prepare catalysts of comparable surface Au densities. The comparison reveals differences in the pathways for introduction of oxygen into CO oxidation reaction. Au on reducible $FePO_4$ catalyzes CO oxidation through both a direct pathway and by a redox pathway in which O from the $FePO_4$ lattice participates in CO oxidation. We now find that Au on non-reducible $LaPO_4$ also catalyzes CO oxidation through a direct pathway, but in addition, surface hydroxyls are found to be active for reacting with CO. The pathway may involve a carboxyl intermediate that is proposed on other Au catalysts and for water–gas shift reaction. The evidence for a hydroxyl-mediated pathway in $Au/LaPO_4$ is evolution of CO_2 during CO adsorption and co-production of CO_2 and H_2 during TPR and isotope labeling adsorption studies. Although hydroxyls can provide active O by reaction with CO, the $LaPO_4$ is fundamentally non-reducible as proven in H_2-TPR and consistent with the absence of Raman signature of reduction. The two different pathways are also linked to differences in the charge state of the Au, indicated by the CO linear peak position in DRIFTS. For $Au/LaPO_4$, no cationic Au is observed (unlike $Au/FePO_4$), but metallic Au is present after both oxidative and reductive treatment. In addition, metallic Au on $LaPO_4$ is accompanied by anionic Au (not seen on $Au/FePO_4$) that accumulates during CO exposure, even after an oxidative pretreatment. The activities of the Au catalysts on the two supports are roughly comparable when the Au is in metallic form. However, the activity of the $Au/FePO_4$ is distinctly lower after oxidative treatment, due to less active cationic Au. In spite of these support differences and three different pathways identified to be contributing, in the end, the most important reaction pathway appears to be direct reaction pathway catalyzed on reduced Au.

Acknowledgments

This research was sponsored by the Division of Chemical Sciences, Geosciences, and Biosciences, Office of Basic Energy Sciences, US Department of Energy. A portion of this research was performed using facilities at Oak Ridge National Laboratory's Center for Nanophase Materials Sciences, sponsored by the Scientific User Facilities Division, Office of Basic Energy Sciences, US Department of Energy. Meijun Li was sponsored by an appointment to the Oak Ridge National Laboratory Postdoctoral Research Associates Program administered jointly by the Oak Ridge Institute for Science and Education and Oak Ridge National Laboratory.

Appendix A. Supplementary material

Supplementary data associated with this article can be found, in the online version, at doi:10.1016/j.jcat.2010.11.019.

References

[1] G.C. Bond, D.T. Thompson, Catal. Rev. Sci. Eng. 41 (1999) 319–388.
[2] R.M.T. Sanchez, A. Ueda, K. Tanaka, M. Haruta, J. Catal. 168 (1997) 125–127.
[3] W.L. Deng, C. Carpenter, N. Yi, M. Flytzani-Stephanopoulos, Top. Catal. 44 (2007) 199–208.
[4] A.A. El-Moemen, G. Kucerova, R.J. Behm, Appl. Catal. B – Environ. 95 (2010) 57–70.
[5] C. Ratnasamy, J.P. Wagner, Catal. Rev. Sci. Eng. 51 (2009) 325–440.
[6] D.T. Thompson, Top. Catal. 38 (2006) 231–240.
[7] X.Y. Deng, B.K. Min, A. Guloy, C.M. Friend, J. Am. Chem. Soc. 127 (2005) 9267–9270.
[8] R. Meyer, C. Lemire, S.K. Shaikhutdinov, H. Freund, Gold Bull. 37 (2004) 72.
[9] J. Kim, Z. Dohnalek, B.D. Kay, J. Am. Chem. Soc. 127 (2005) 14592–14593.
[10] J.D. Henao, T. Caputo, J.H. Yang, M.C. Kung, H.H. Kung, J. Phys. Chem. B 110 (2006) 8689–8700.
[11] J.C. Clark, S. Dai, S.H. Overbury, Catal. Today 126 (2007) 135–142.
[12] J.T. Calla, R.J. Davis, J. Catal. 241 (2006) 407–416.
[13] N. Lopez, T.V.W. Janssens, B.S. Clausen, Y. Xu, M. Mavrikakis, T. Bligaard, J.K. Nørskov, J. Catal. 223 (2004) 232–235.
[14] N. Lopez, J.K. Nørskov, J. Am. Chem. Soc. 124 (2002) 11262–11263.
[15] S.H. Overbury, V. Schwartz, D.R. Mullins, W.F. Yan, S. Dai, J. Catal. 241 (2006) 56–65.
[16] M.S. Chen, D.W. Goodman, Science 306 (2004) 252–255.

[17] S.N. Rashkeev, A.R. Lupini, S.H. Overbury, S.J. Pennycook, S.T. Pantelides, Phys. Rev. B 76 (2007) 035431–035438.
[18] A.A. Gokhale, J.A. Dumesic, M. Mavrikakis, J. Am. Chem. Soc. 130 (2008) 1402–1414.
[19] C.K. Costello, M.C. Kung, H.-S. Oh, Y. Wang, H.H. Kung, Appl. Catal. A – Gen. 232 (2002) 159–168.
[20] C.K. Costello, J.H. Yang, H.Y. Law, Y. Wang, J.N. Lin, L.D. Marks, M.C. Kung, H.H. Kung, Appl. Catal. A – Gen. 243 (2003) 15–24.
[21] M.C. Kung, R.J. Davis, H.H. Kung, J. Phys. Chem. C 111 (2007) 11767–11775.
[22] M.M. Schubert, S. Hackenberg, A.C. van Veen, M. Muhler, V. Plzak, R.J. Behm, J. Catal. 197 (2001) 113–122.
[23] J.A. Rodriguez, L. Feria, T. Jirsak, Y. Takahashi, K. Nakamura, F. Illas, J. Am. Chem. Soc. 132 (2010) 3177–3186.
[24] L.K. Ono, B. Roldan-Cuenya, Catal. Lett. 113 (2007) 86–94.
[25] Z. Ma, S. Brown, S.H. Overbury, S. Dai, Appl. Catal. A – Gen. 327 (2007) 226–237.
[26] Z. Ma, H. Yin, S.H. Overbury, S. Dai, Catal. Lett. 126 (2008) 20–30.
[27] W.F. Yan, S. Brown, Z.W. Pan, S.M. Mahurin, S.H. Overbury, S. Dai, Angew. Chem. Int. Ed. 45 (2006) 3614–3618.
[28] M. Li, Z. Wu, Z. Ma, V. Schwartz, D. Mullins, S. Dai, S.H. Overbury, J. Catal. 266 (2009) 98–105.
[29] P. Nagaraju, C. Srilakshmi, N. Pasha, N. Lingaiah, I. Suryanarayana, P.S.S. Prasad, Appl. Catal. A – Gen. 334 (2008) 10–19.
[30] F. Boccuzzi, A. Chiorino, M. Manzoli, Surf. Sci. 454–456 (2000) 942–946.
[31] M. Manzoli, F. Boccuzzi, A. Chiorino, F. Vindigni, W.L. Deng, M. Flytzani-Stephanopoulos, J. Catal. 245 (2007) 308–315.
[32] F. Menegazzo, M. Manzoli, A. Chiorino, F. Boccuzzi, T. Tabakova, M. Signoretto, F. Pinna, N. Pernicone, J. Catal. 237 (2006) 431–434.
[33] Z. Wu, S. Zhou, H. Zhu, S. Dai, S.H. Overbury, Chem. Commun. 2008 (2008) 3308–3310.
[34] K.I. Hadjiivanov, G.N. Vayssilov, Adv. Catal., vol. 47, Academic Press Inc., San Diego, 2002.
[35] W.C. Conner Jr., J.L. Falconer, Chem. Rev. 95 (1995) 759.
[36] J.A. Rodriguez, P. Liu, J. Hrbek, J. Evans, M. Perez, Angew. Chem. Int. Ed. 46 (2007) 1329–1332.
[37] Q. Yuan, Q.H. Zhang, Y. Wang, J. Catal. 233 (2005) 221–233.
[38] G. Fröhlich, W.M.H. Sachtler, J. Chem. Soc. Faraday Trans. 94 (1998) 1339.
[39] G. Deganello, F. Giannici, A. Martorana, G. Pantaleo, A. Prestianni, A. Balerna, L.F. Liotta, A. Longo, J. Phys. Chem. B 110 (2006) 8731.
[40] E. Muneyama, A. Kunishige, K. Ohdan, M. Ai, J. Catal. 158 (1996) 378–384.
[41] S.C. Chang, A. Hamelin, M.J. Weaver, Surf. Sci. 239 (1990) L543.
[42] K. Kunimatsu, A. Aramata, H. Nakajima, H. Kita, J. Electrananl. Chem. 207 (1986) 293.
[43] Y. Park, B. Lee, C. Kim, J. Kim, S. Nam, Y. Oh, B. Park, J. Phys. Chem. B 114 (2010) 3688–3692.
[44] A. Fukuoka, J. Kimura, T. Oshio, Y. Sakamoto, M. Ichikawa, J. Am. Chem. Soc. 129 (2007) 10120.